Optimal Design of Standalone Photovoltaic System Based on Multi-Objective Particle Swarm Optimization: A Case Study of Malaysia

Authors:

Hussein Mohammed Ridha, Chandima Gomes, Hashim Hizam, Masoud Ahmadipour

Date Submitted: 2020-02-03

Keywords: levelized cost of energy (LCE), loss of load probability (LLP), life cycle cost (LCC), Particle Swarm Optimization, multi-objective optimization, standalone PV system

Abstract:

This paper presents a multi-objective particle swarm optimization (MOPSO) method for optimal sizing of the standalone photovoltaic (SAPV) systems. Loss of load probability (LLP) analysis is considered to determine the technical evaluation of the system. Life cycle cost (LCC) and levelized cost of energy (LCE) are treated as the economic criteria. The two variants of the proposed PSO method, referred to as adaptive weights PSO (A W P S O c f) and sigmoid function PSO (S F P S O c f) , are implemented using MATLAB software to the optimize the number of PV modules in (series and parallel) and number of the storage battery. The case study of the proposed SAPV system is executed using the hourly meteorological data and typical load demand for one year in a rural area in Malaysia. The performance outcomes of the proposed A W / S F P S O c f methods give various configurations at desired levels of LLP values and the corresponding minimum cost. The performance results showed the superiority of S F P S O c f in terms of accuracy is selecting an optimal configuration at fitness function value 0.031268, LLP value 0.002431, LCC 53167 USD, and LCE 1.6413 USD. The accuracy of A W / S F P S O c f methods is verified by using the iterative method.

Record Type: Published Article

Submitted To: LAPSE (Living Archive for Process Systems Engineering)

Citation (overall record, always the latest version):	LAPSE:2020.0153
Citation (this specific file, latest version):	LAPSE:2020.0153-1
Citation (this specific file, this version):	LAPSE:2020.0153-1v1

DOI of Published Version: https://doi.org/10.3390/pr8010041

processes

MDPI

Article

Optimal Design of Standalone Photovoltaic System Based on Multi-Objective Particle Swarm Optimization: A Case Study of Malaysia

Hussein Mohammed Ridha [1,2,*], Chandima Gomes [3], Hashim Hizam [1,2] and Masoud Ahmadipour [1,2]

1 Department of Electrical and Electronic Engineering, Universiti Putra Malaysia, Serdang 43400, Malaysia; hhizam@upm.edu.my (H.H.); maseod.ahmadipour@gmail.com (M.A.)
2 Advanced Lighting and Power Energy Research (ALPER), Universiti Putra Malaysia, Serdang 43400, Malaysia
3 School of Electrical and Information Engineering, University of Witwatersrand, 1 Jan Smuts Avenue, Braamfontein, Johannesburg 2000, South Africa; chandima.gomes@wits.ac.za
* Correspondence: hussain_mhammad@yahoo.com

Received: 9 October 2019; Accepted: 19 November 2019; Published: 1 January 2020

Abstract: This paper presents a multi-objective particle swarm optimization (MOPSO) method for optimal sizing of the standalone photovoltaic (SAPV) systems. Loss of load probability (LLP) analysis is considered to determine the technical evaluation of the system. Life cycle cost (LCC) and levelized cost of energy (LCE) are treated as the economic criteria. The two variants of the proposed PSO method, referred to as adaptive weights PSO ($AWPSO_{cf}$) and sigmoid function PSO ($SFPSO_{cf}$), are implemented using MATLAB software to the optimize the number of PV modules in (series and parallel) and number of the storage battery. The case study of the proposed SAPV system is executed using the hourly meteorological data and typical load demand for one year in a rural area in Malaysia. The performance outcomes of the proposed $AW/SFPSO_{cf}$ methods give various configurations at desired levels of LLP values and the corresponding minimum cost. The performance results showed the superiority of $SFPSO_{cf}$ in terms of accuracy is selecting an optimal configuration at fitness function value 0.031268, LLP value 0.002431, LCC 53167 USD, and LCE 1.6413 USD. The accuracy of $AW/SFPSO_{cf}$ methods is verified by using the iterative method.

Keywords: standalone PV system; multi-objective optimization; particle swarm optimization; life cycle cost (LCC); loss of load probability (LLP); levelized cost of energy (LCE)

1. Introduction

Ever-raising energy load demands, the depletion of the fossil fuel resources, and the global warming encourage energy system designers to optimize their designs. Photovoltaic (PV) systems can be categorized into three types based on the approach of utilization, namely, SAPV system, grid-connected PV system, and hybrid PV system, respectively [1–3]. The use of standalone PV (SAPV) systems can lead to a transformation of technology in terms of "leaving the grid" or "living in off-grid". Furthermore, the risk of increasing electricity bills and tariffs will not affect the customers that have gone off the utility grid [4,5]. However, the expensive cost and limited energy conversion efficiency of the PV modules are the major obstacles of the SAPV system. Thus, an appropriate design of a SAPV system is required to fulfill the load demand.

The performance of SAPV system strongly depends on availability of the meteorological data such as solar irradiation and ambient temperature, load demand, and the associated components. Techno-economic criteria must be considered at specific levels of reliability with a lower cost. Different

methodologies have been employed in literature for designing SAPV systems such as intuitive, analytical, numerical, and artificial intelligence, and hybrid methods [6–8]. In the intuitive method, the nonlinearity between various sub-systems is ignored. Moreover, the intuitive method uses simple meteorological data such as worst monthly average, monthly solar irradiation or average annual which may result in an undesired design of the system. The safety factor is selected during the designing period by the designers' experience when the output energy of the PV system is met or raised the load demand [9]. The optimal size in Ref. [9] is chosen based on economic parameter life cycle cost (LCC) and energy payback time (EPBT) without considering the reliability of the system which is recommended to give initial approximation of the PV system. As an example, Abdul et al. [10] presented an optimal size of a SAPV system in Pakistan, where the annualized life cycle cost (ALCC) was obtained as the economic criteria. The reliability criteria has not been mentioned in this study. The monthly average daily solar irradiance has been used which can result over/under sizing of the PV system. In meanwhile, an analytical method has been considered to correlate the cost and availability of the system. The size of standalone PV system in this method is calculated by the driving equations. However, the main obstacle is the complexity in computing the coefficients of the equations of PV system which are strongly location dependent [11]. In another case, Marco et al. [12] presented a techno-economic model to optimally optimize the size of a PV/battery combination with grid-connected system. The hourly meteorological data and load demand distribution have considered in this study as the input parameters. State of charge (SOC) was used as an objective function, whereas, LCE was used as an economic criterion. In addition to that, the authors of [13] have investigated six outdoor solar air conditioners with various sizes of PV panels. A small buffer battery has been used to reduce the cost and to meet the demand energy. The Loss of power (LL) has been utilized for evaluating the reliability without considering the cost of the system. The numerical method is considered to be an accurate method and could overcome the drawbacks of intuitive and analytical methods. However, it takes a comparatively long execution time. In fact, a design space of the numerical method contains various configurations of the SAPV system. Each configuration is simulated using hourly meteorological data and typical load demand at specific level of reliability. Then, the cost is calculated for the configurations that meet desired reliability of the system. The lower configuration cost with favourable level of reliability is chosen as an optimal design [14]. Numerous studies based on iterative method can be reviewed in the literature. Stefano et al. [15] proposed a numerical sizing methodology for off-grid PV system using daily average meteorological data in a remote area in Uganda. SOC for each step time and LL during the discharge were used as technical criteria. The value of lost load (VOLL), levelized cost of supplied and lost energy (LCoSLE) were considered as economic criteria. The authors of [16] have proposed a sizing methodology of the standalone PV system in Malaysia. Loss of power supply probability (LPSP) was chosen as the technical criteria and LCE as the economic criteria by considering amp-hour analysis. However, a linear PV model has been used in this study. Ameen et al. [17], presented an improved iterative method for finding an optimal configuration of SAPV system in Yemen. LLP was used as technical criteria and the NPC has been considered as the economic criteria. Hourly meteorological data and typical load demand were obtained in this study. However, a simple PV model has been used in the prediction the output power energy. A dynamic model of storage battery and accurate estimation of SOC are required in sizing of SAPV system to increase the life time and reducing its replacing time which can decrease the capital cost of the system [18,19].

Recently, artificial intelligence (AI) methods have been extensively applied to find the sizing of SAPV systems. This may be due to the improved accuracy and reduced execution time of AI methods. Furthermore, the ability of AI systems such as genetic algorithm (GA) [20], artificial bee colony (ABC) [21], generalized artificial neural network (GRNN) [22], fuzzy logic [23], firefly methods (FL) [24], and particle swarm optimization (PSO), to cope up with missing meteorological data, is a significant advantage. However, the complexity in designing of an SAPV system is the main drawback of AI methods. The authors of [20] proposed GA to optimize the size of remote PV systems based on synthetic hourly meteorological data, in Adrar city in South Algeria. In [20], the capital cost

of the system was employed as an objective function without considering the availability of the system. However, the proposed GA compared with LPSP method and worst month method based on cost criteria. The results showed the superiority of the GA method. Chokri et al. [23] presented FL method to supply energy for a SAPV system in Safax, in the coast of Tunisia. Monthly average of the daily solar radiation was utilized as input of the proposed sizing algorithm. However, the cost and level of reliability of the system have not been mentioned. Moreover, the authors of [22] proposed GRNN method to predict optimal size of the a SAPV system in five Malaysian sites. Hourly meteorological data and load demand were used in this study. However, the proposed GRNN has been evaluated based on a single objective function which is the loss of load probability (LLP). Finally, Nur et al. [24] proposed firefly algorithm sizing algorithm (FLSA) for sizing of a SAPV system. LPSP was used as a technical parameter whereas the economic parameter was not mentioned. The FLSA was found faster than PSO, evolutionary programming (EP) and GA. Some of software tools have been utilized for sizing of a SAPV system based on economic evaluation, and planning and analysis tools such as PV.sys, Transient System Simulation (TRNSYS), Hybrid Optimization Model for Electrical Renewable (Homer), improved Hybrid Optimization by Genetic Algorithm (iHOGA), RetScreen, and System Advisor Model (SAM) [25]. Several studies have employed hybrid methods by combining two methods or more to find an optimal design of the SAPV system [26–29]. The hybrid methods overcome the drawbacks of AI methods by high ability of convergence to optimal solutions and reducing the execution time. In [30], a hybrid method was proposed to optimal size of a SAPV system by using differential evolution multi-objective optimization (DEMO) and multi-criteria decision making (MCDM). Set of configurations were conducted by using DEMO algorithm. Then, AHP and TOPSIS were obtained to select optimal configuration. Techno-economic criteria for minimizing two objectives was utilized to describe the performance of the proposed method. However, the complexity is one of the drawbacks of the proposed method. Furthermore, the numbers of series PV and battery are assumed to be constant during the optimization. Fabian et al. [31] proposed a computational method for designing off-grid SAPV system by analysing the suppressed demand (SD) effect in south-west highlands, Bolivia. Three types of electrical load profiles were used based on simulated geographical data. The LPSP was employed as technical evaluation using two different capacity of the lithium-ion battery. Whist, the cost of the components of the system was set at 2.5 USD/Wp. The major drawback of the proposed method in Ref. [31] is by supplying the required load demand only by energy conducted from storage battery. This will lead not only increasing the replacements of the storage battery but also raising the cost of the system.

Based on the reviewed literature, multi-objective PSO (MOPSO) method has been not applied based on three conflicts objectives for SAPV systems. The two variants of MOPSO methods are proposed to overcome the obstacles of accurate results of intuitive and analytical methods as well as the long execution time of the numerical methods. In addition, MOPSO method can deal with three objectives synchronously based on techno-economic criteria. Finally, MOPSO method offers a set of optimal configurations by considering the given priority weights to the individual objectives. Therefore, this methodology intends to suggest optimal number of PV array which comprises of parallel and series PV modules and optimal number of storage battery. The technical criteria is calculated according to the method of the loss of load probability (LLP) and the economic criteria is computed according to the method of life cycle cost (LCC) and levelized cost of energy (LCE). The three conflicting objectives: LLP, LCC, and LCE are weighted, normalized, and then aggregated by a mono-objective function which is required to be minimized to select an optimal solution as the best solution. The performance of the proposed $AW/SFPSO_{cf}$ are analysed using hourly meteorological data and typical load demand. The validation of the two variation of PSO algorithms are verified by using numerical method. The rest of the paper is organized as follow. Section 2 presents the definitions, concepts, steps of modeling the SAPV systems. The techno-economic evaluations criteria of the SAPV system are given in Section 3. The particle swarm optimization and the details of the proposed multi-objective optimization approach

are given in Section 4. Section 5 explains the energy flow modeling for SAPV system. Section 6 presents the results and discussions. Finally, Section 7 concludes the work and suggests future directions.

2. The SAPV System Modelling

A common a SAPV system comprises of four main parts, namely, PV array which comprises numbers of parallel and series PV modules, DC-DC converter, battery storage, and DC-AC inverter. The PV arrays convert the sunlight into DC current, the storage battery stores the excess energy and the power electronics invert DC into AC [10,32]. Figure 1 illustrates the block diagram of a SAPV system.

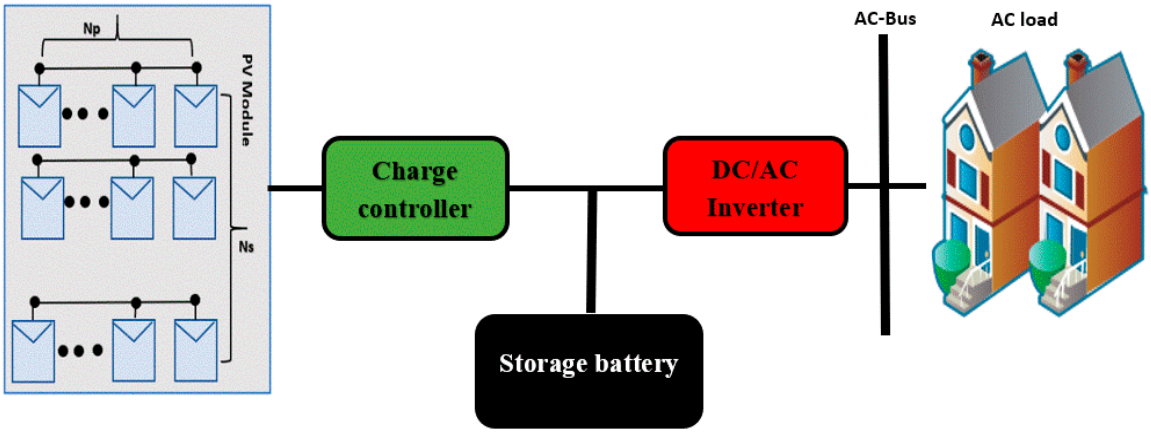

Figure 1. The block diagram of a generalized standalone photovoltaic (SAPV) system.

2.1. Single Diode (SD) Model

The single-diode PV model offers high ability in reflecting the reality behavior when it is dealing with non-linearity and stochastic nature among other mathematical models [33]. The electrical equivalent circuit of a single-diode (SD) PV module model is shown in Figure 2. The circuit comprises an ideal dependent current source, which is the photocurrent (I_{Ph}) of solar cell and has high sensitivity to randomly nature of the meteorological data. Furthermore, the output voltage of the solar cell is given by the connection of the parallel reverse mode diode with the current source. Parallel resistance and R_s represent the losses of the PV solar cell. Therefore, the output current of the PV solar cell is represented by the following equation:

$$I = I_{Ph} - I_o\left[exp\left(\frac{V + IR_s}{V_t}\right) - 1\right] - \frac{V + IR_s}{R_p} \quad (1)$$

where I_{Ph} refers to the photocurrent, I_o denotes the diode reverse saturation currents of the diode (in A), R_s and R_p are the series and shunt resistances (in Ω), respectively, V is output voltage (in V) and I is output current (in A) of the solar cell, respectively, and V_t represents the diode thermal voltage (in V) which is given by,

$$V_t = \frac{dKBT_c}{q} \quad (2)$$

where d refers to the diode ideality factor that represents the diffusion current's components, KB is the Boltzmann's constant (1.3806503×10^{-19} J/K), T_c represents the cell temperature (K) and q refers to the electron charge (1.60217646×10^{-19} Coulombs) where I_{Ph}, I_o, R_s, R_p and d of Equation (1) are the five parameters that require great computations efforts to be extracted. These five parameters can also be sensitive to the operational conditions.

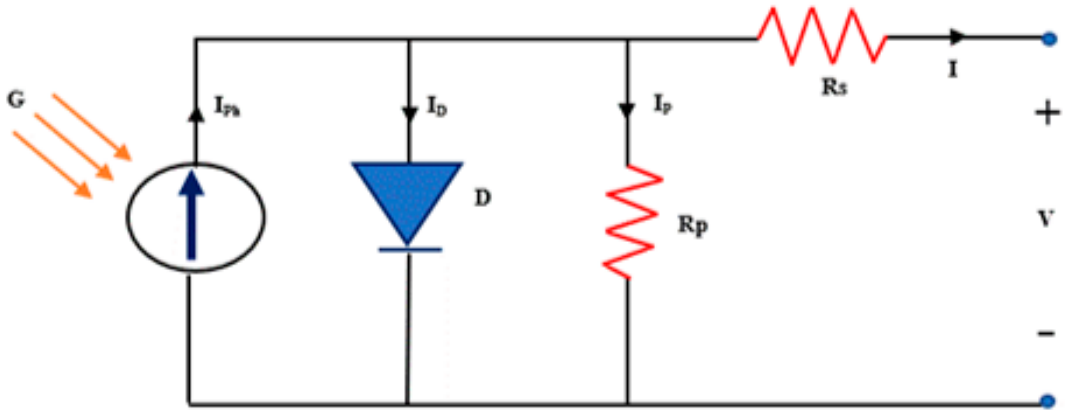

Figure 2. Solar cell of a single-diode electrical circuit.

The PV array comprises of series N_p and parallel N_s modules, respectively. Therefore, the PV array's output current can be expressed as follows:

$$I = N_p I_{Ph} - N_p I_0 \left[exp\left(\frac{1}{V_t} \left(\frac{V}{N_s} + \frac{IR_s}{N_p} \right) \right) - 1 \right] - \frac{N_p}{R_p} \left(\frac{V}{R_p} + \frac{IR_s}{N_p} \right), \tag{3}$$

where; I_{Ph}, I_0, R_s, R_p and d of Equation (1) are the five parameters that extracted by the proposed Improved electromagnetism-like algorithm (IEM) algorithm the output I-V and P-V characteristics curves are shown in Figure 3a,b, V, I are the output voltage (A) and current (V) of the PV array, respectively.

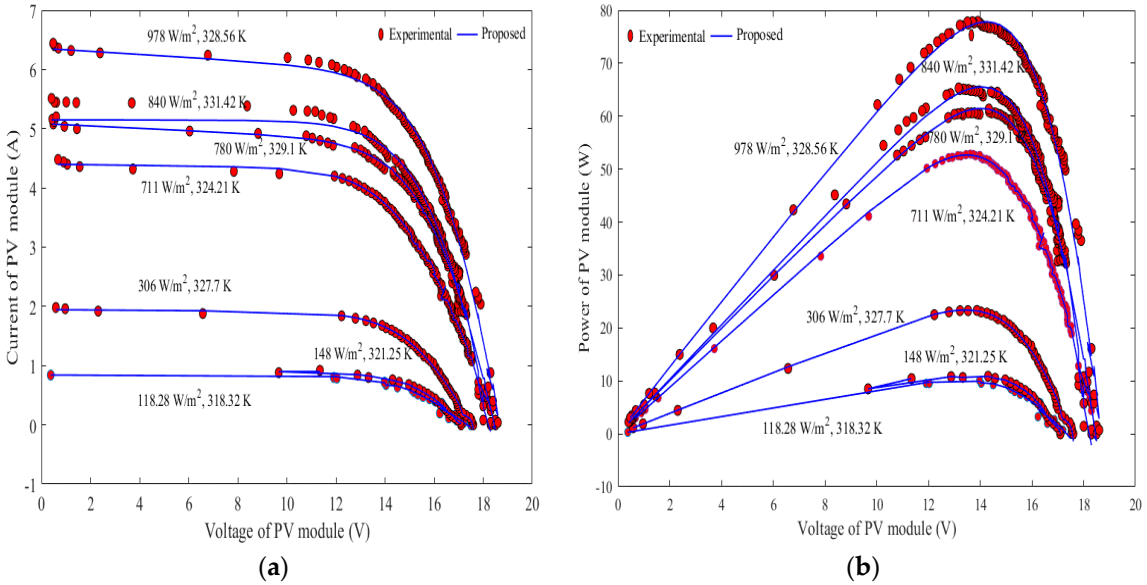

Figure 3. Photovoltaic (PV) characteristics under various cell temperature and solar radiation of improved electromagnetism (IEM) algorithm (**a**) (I-V) curves and (**b**) (P-V) characteristics curves.

The PV array's efficiency can be calculated as follows:

$$\eta_{PV} = \frac{VI}{AG_T} \tag{4}$$

where G_T is the amount of the solar irradiation fall on the PV array surface W/m^2 and A represents the PV array's area. Kyocera (KC120-1) multi-crystalline silicon PV module are utilized in this study.

The PV module's specification under standard test condition (STC) are given in Table 1. It's important to notice that the parameters of SD PV model using IEM algorithm were extracted at maximum power point (MPP) which cannot translate the actual performance of the PV system. Thus, it needs to shift to applicable irradiance and temperature levels such as: 840 (W/m^2) and 32.170 °C, respectively. Chenlo et al. [34] used five equations for translation curve from MPP to any new point. The root mean square error (RMSE) difference value between the measurement and simulation data was found 1% by Hadj Arab et al. [35]. However, the used equations in [34,35] distorted the shape of simulated new point of the I-V curve and the simulation results demonstrated that solely two equations are required to establish the I-V curve at under any weather conditions:

$$I_{sc}(S,T) = I^*_{sc}\frac{G}{G^*} + \alpha(T - T^*), \tag{5}$$

$$V_{oc}(S,T) = V_{oc} - \beta(T - T^*)\frac{G}{G^*} + \eta V_t \ln\left(\frac{G}{G^*}\right), \tag{6}$$

Table 1. Standalone photovoltaic (SAPV) system's key specification [36].

Components	Characteristics	Value
Kyocera *KC*120-1 PV panels	Maximum power at STC	120 (W)
	Open circuit voltage	21.5 (V)
	Short circuit current	7.45 (A)
	Voltage at MPP	16.9 (V)
	Current at MPP	7.1 (A)
	No. of cells connected in series	36
	Nominal operation cell temperature	43.6 (°C)
Battery	Lead acid	
	Efficiency	85%
	Capacity	220 Amp-hours
	Maximum *DoD*	80%
	Bus voltage	24 (V)
	Battery voltage	6 (V)
Charge controller PS-MPPT-40	Efficiency	95%
Inverter	Efficiency	90%
AC voltage	Electrical load AC	230 (V)

2.2. Mathematical Model of the Battery

The storage battery capacity (kW) is simulated considering the required load demand and the days of the autonomy which can be given by [37],

$$C_{bat} = \frac{E_{Load} * AD}{DOD * \eta b * \eta inv} \tag{7}$$

where E_{Load} is the load demand, AD is the autonomy days (typically 3–5 days) [38], DOD is the depth of discharge (80%), $\eta b * \eta inv$ are the battery (85%) and inverter efficiencies (95%).

On the other hand, the state of chare of the storage battery (SOC) is modeled as the following [16]:

$$E_{bat} = SOC(t-1) + \left[P_{pv}(t) - P_{load}(t)\right] \tag{8}$$

$$SOC(t) = \begin{cases} SOC_{min}\,, E_{bat} < SOC_{min} \\ E_{bat}\,, SOC_{min} < E_{bat} < SOC_{max} \\ SOC_{max}\,, E_{bat} > SOC_{max} \end{cases} \tag{9}$$

where $SOC(t)$ and $SOC(t-1)$ represent the SOC for the storage battery at final and initial points of charging and discharging, respectively, and E_{bat} refers to hourly capacity of the battery.

The minimum energy in the storage battery can be written as:

$$E_{bat\_min} = SOC_{max} * (1 - DOD) \tag{10}$$

The annual amount of energy considered to be stored in storage battery can be given by [38],

$$E_{bat} = \left(\sum_{i=1}^{365} energy\ excess - \sum_{i=1}^{365} energy\ deficit \right). \eta ch \tag{11}$$

where ηch denotes to the storage battery's charging efficiency.

3. Evaluations Criteria for the Sizing of Standalone PV System

In SAPV system, the chosen optimal configuration can significantly affect the performance of the system to meet the required load demand. In this case study, the optimal configuration is based on minimizing three objectives, namely, loss of load probability (LLP), life cycle cot (LCC), and levelized cost of energy (LCE).

3.1. Loss of Load Probability (LLP)

The LLP indicates the availability of standalone PV/battery system. It can be defined as the ratio of annual energy deficits to annual required load demands throughout specific time period [39], the LLP is expressed as below:

$$LLP = \frac{\sum_{1}^{12*365} Energy\ deficits_i}{\sum_{1}^{12*365} Energy\ demand_i}, \tag{12}$$

3.2. Life Cycle Cost (LCC)

The life cycle cost (LCC) of the SAPV system is considered in this research work to be the best criteria of economic profitability of the system cost analysis, following the outcomes of previous research. The LCC can be defined as the total cost of the all components of the standalone PV system. There are four main parts proposed in this system: PV array, storage battery, bidirectional converter, and charge regulator. The LCC takes into calculation the initial capital cost $\left(IC_{cap}\right)$, the present value of replacement cost $\left(C_{rep}\right)$, and the present value of operation and maintenance cost $(C_{O\&M})$. The lifetime and unit cost of the system's components are tabulated in Table 2. Therefore, the mathematical equation can be written as [21]:

$$LCC = IC_{cap} + C_{rep} + C_{0\&M}, \tag{13}$$

The initial capital cost of each part of the system components is taken into account which comprises of the component price, installation, and the cost of civil works. The initial cost of the off-grid SAPV system $\left(IC_{cap}\right)$ is given by [40]:

$$IC_{cap} = C_{PV} \times C_{Unit,PV} + C_{Batt} \times C_{Unit,Batt} + C_{Bidi} \times C_{Unit,Bidi} + C_{CH} \times C_{Unit,CH} + C_O, \tag{14}$$

where C_{PV},$C_{Unit,PV}$ represent the total capacity (W) and unit cost ($/W) of the PV array, respectively; C_{Batt}, $C_{Unit,Batt}$ represent the total capacity (W) and unit cost ($/W) of the battery, respectively; C_{Bidi},$C_{Unit,Bidi}$ represent the total capacity (W) and unit cost ($/W) of bidirectional inverter, respectively; C_{CH},$C_{Unit,CH}$ represent the total capacity (W) and unit cost ($/W) of the charge regulator, respectively; and (C_O) represents the total constant cost including both civil work and installation cost.

The present value of the replacement cost of each part of the system component is defining as the present value of all the replacement costs during the system lifetime. Since the lifetime of the storage battery, charge controller, and the bidirectional inverter are shorter than PV arrays, the replacement cost of the components of the SAPV system with the inflation rate (FR) and the real interest rate

of components replacements (IR) are included in this calculation. Therefore, the present value of replacement cost (C_{rep}) can be described as [40];

$$C_{rep} = C_{Unit} \times C_{nom}\left(\sum_{i=1}^{N_{rep}}\left[\frac{1+FR}{1+IR}\right]\right)^{\left(\frac{LP*i}{Nrep+1}\right)}, \quad (15)$$

where C_{Unit} is unit component cost of storage battery in ($/W), charge regulator in ($/W) and bidirectional inverter in ($/W); ($C_{nom}$) is the nominal capacity of the replacement system component such as storage battery in (Wh), charge controller in (W) and the bidirectional inverter in (W), and (N_{rep}) is the number of replacement of each component over the system life period (LP).

The calculation of the present value of operation and maintenance cost ($C_{O\&M}$) of the standalone PV system can be expressed as [41]:

$$C_{O\&M} = \begin{cases} C_{O\&MO}\left(\frac{1+FR}{IR-FR}\right)\left(1-\left[\frac{1+FR}{IR+FR}\right]^{LP}\right) for\ IR \neq FR \\ C_{O\&MO} \times LP\ for\ IR = FR \end{cases} \quad (16)$$

where $C_{O\&M0}$ represents the operation and maintenance cost in the first year in ($). The financial data of the proposed SAPV system are given in Table 2 [26,42].

Table 2. Shows the unit cost for standalone PV system's components [26,43].

Components	Cost/Unit	Lifetime (in Year)	*O&M*	Nrep	IR	FR	LP
PV array	1 $/Wp	20	1%	0	0.08	0.04	20
Charge controller	0.5 $/Wp	10	0%	1			
Storage battery	0.118 $/Wp	2	5%	10	Replacement cost		0.0042
Inverter	0.5 $/Wp	10	0%	1			

3.3. Levelized Cost of Energy (LCE)

The third parameter to represent the economic aspects is levelized cost of energy (LCE) which refers to the ratio of the total cost of the system's component to the total energy conducted by a SAPV system during specific period of time, and it is expressed as following [44,45],

$$LCE = \frac{TAC}{E_{total}} \quad (17)$$

where; TAC represents the total annual cost of the system components and can be expressed as:

$$\text{TAC} = (\text{LCC/LP}) \quad (18)$$

E_{total} represents the total energy conducted by a SAPV system during specific life period.

4. Multi-Objective Particle Swarm Optimization (MOPSO)

The particle swarm optimization (PSO) algorithm is a stochastic optimization technique population-based search to choose the optimal solutions. It was developed in 1995 by Eberhart and Kennedy [46] who have been inspired by the social behavior of the bird flocking and fish schooling. PSO algorithm has several advantages such as; it can easily be programmed, shorter calculation time with high ability of convergence to the optimal values, and robustness to control parameters [47,48]. PSO algorithm presents high convergence rate for single-objective function and can be powerful in finding the Pareto front in multi-objective optimization [49].

In PSO algorithm, the group of random parameters are initiated (search space) to search the optimal parameter values by updating in each generation. At each iteration, a particle is developed by two values which are individual best and global best. The individual best is the best solution achieved by the particle. The global best is the best value obtained among the population in all previous iterations. Each particle has a position which represents the value of the variables and a velocity that moves the direction towards the individual and global bests. The fitness function (f) is used to select the best solution from all feasible solutions. In this study, the fitness function is given by obtaining the minimum values of LLP, LCC and LCE. The PSO algorithm comprises of the following steps (see Figure 4).

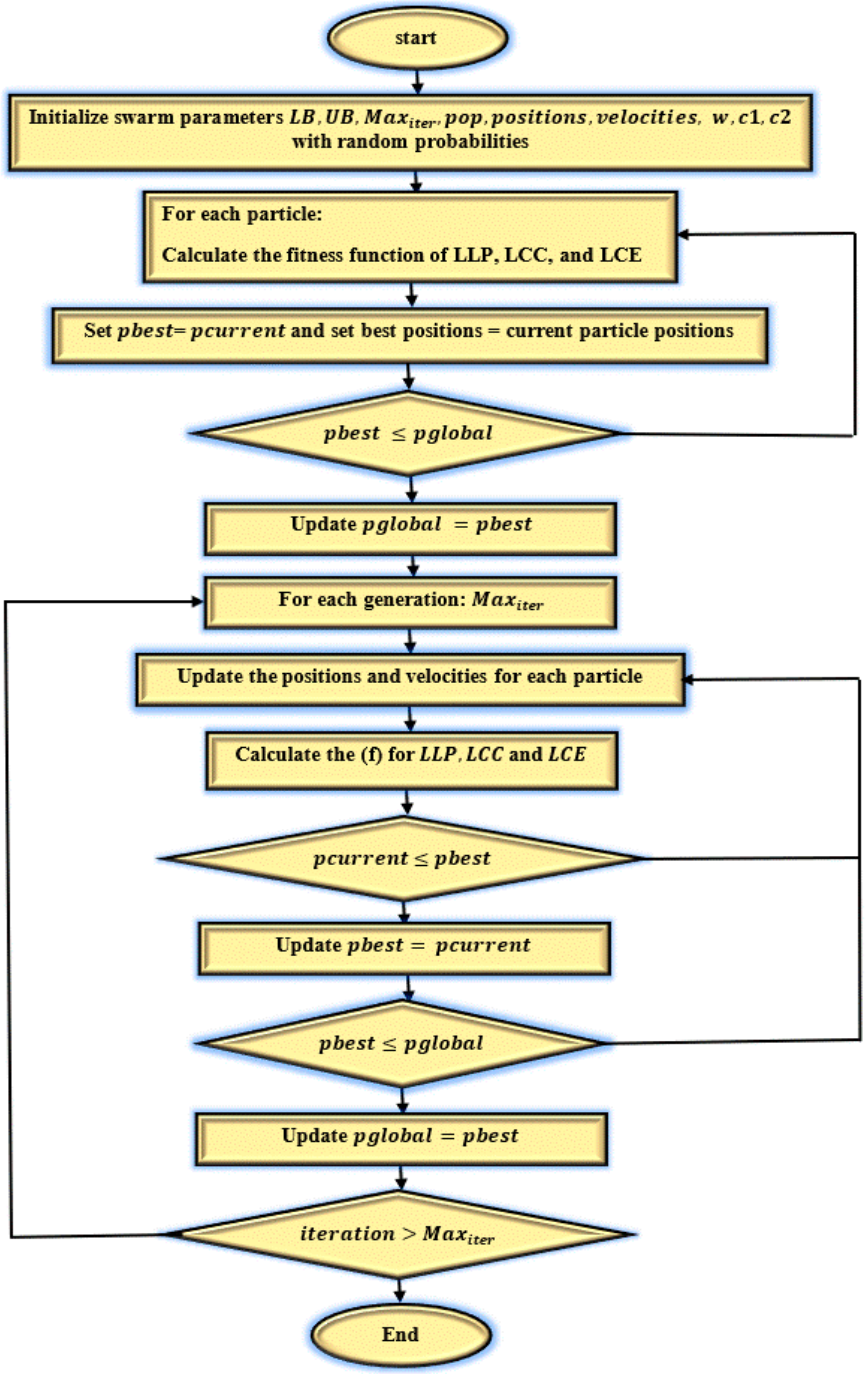

Figure 4. Flow chart of the proposed optimal sizing of SAPV system using $AW/SFPSO_{cf}$ method.

Step 1: initialization

The variables of the PSO algorithm are valued and the m particles are initialized in the predetermined range of the search space. After that, the fitness function for each particle is calculated.

Step 2: updating the individual and global best

The particle who has best fitness function is chosen as optimal value and stored in *pbest* and *gbest* is chosen among the population and updating during iterations.

Step 3: updating the velocity and position

The particle's velocity and position in the population is updated using the following equations:

$$x_i^G = x_i^G + v_{i+1}^G \tag{19}$$

where x denotes to particle position and v represents the velocity of the particle in the iteration i. The velocity v is given by the following:

$$v_{i+1}^G = w * \left[v_i^G + c_1 r_1 \left(p_i^G - x_i^G \right) + c_2 r_2 \left(p_i^g - x_i^G \right) \right] \tag{20}$$

where p^G represents the best individual particle position and p^g is defined as the best global particle position, c_1 and c_2 represent the learning factors which control the individual and global bests. r_1 and r_2 are uniform numbers between 0 and 1. v_i^G is called inertia and it moves the particle in the same direction with its velocity, $c_1 r_1 \left(p_i^G - x_i^G \right)$ is called cognitive part and this part returns the particle to a previous position which has higher individual fitness, and $c_2 r_2 \left(p_i^g - x_i^G \right)$ is called social part and this part moves the particle to the best region in the population and follows the best direction of the neighbor.

Step 4: checking the feasibility

If the particle exceeds the predetermined range, it will replace by the previous position. The PSO algorithm will stop once the *gbest* is chosen as the best optimal solution. Otherwise, the steps 2–4 are repeated.

In this study, to avoid the premature convergence of the basic particle swarm optimization algorithm, the PSO_{cf} was proposed to provide a better convergence to the optimal solutions. A contraction factor is used to ensure convergence to a stable point, avoiding velocity clamping.

The PSO_{cf} can be expressed by following issue:

$$k = \frac{2}{\left| 2 - \varnothing - \sqrt{\varnothing^2 - 4\varnothing} \right|}, \ \varnothing = c_1 + c_2 \tag{21}$$

4.1. Adaptive Inertia Weight AWPSO$_{cf}$

The value of w determines the overall convergence and exploitation performance of the proposed PSO algorithm. A big search step can speed up the convergence which may skip optimal solutions. In meanwhile, a small search step can ensure a better convergence accuracy. However, the tradeoff between the exploration and exploitation are necessary in designing nonlinear equations. The w value can be represented by follows:

$$w = \frac{2}{1 + \exp\left(\frac{10i}{Max_{iter}} \right)} \tag{22}$$

where i denotes to current number of iterations, Max_{iter} refers to maximum number of generations. From the above equation, the value of w is large at early stage. Then, it decreases as the iteration go on. By this way, the algorithm can hit more accurate solutions at end of iterations.

4.2. A Logistic Sigmoid Function SFPSO$_{cf}$

The second proposed inertia weight uses a logistic sigmoid function which is expressed by the following:

$$w = \frac{l}{1 + \exp(-R(s - s_0))}, \tag{23}$$

where; l represents the maximum value of the curve ($l = 1$), R defines the steepness of the curve, and s_0 describes the sigmoid midpoint on the x-axis ($s_0 = zero$). The differences of the fitness function between the current and previous generations is defined by s which is randomly weighted as expressed by the following:

$$s = rand * \left| f\left(X_{best}^{G}\right) - f\left(X_{best}^{G-1}\right) \right|, \tag{24}$$

where *rand* is randomly selected between the range of [0,1], X_{best}^{G} and X_{best}^{G-1} are the best individual vectors for the current and previous generations, respectively.

In this work, the LLP, LCC, and LCE objectives are converted by aggregation function to a mono-objective which treats the multi-objective optimization problems as a mono-objective problem as written by the following:

$$f_i(x) = \sum_{i=1}^{k} w_i \times f_i(x), \tag{25}$$

where x represents the decision variables vector, which relates to the search space, k that belongs to the individual objective function number and it is an aggregated function. The range of weights coefficients are between $0 > w_i < 1$ which represents the relative importance of the k objective function of the problem and it is assumed as:

$$\sum_{i=1}^{k} w_i = 1, \tag{26}$$

However, the three objective functions are non-scalable. Thus, it's important to normalize and implement the objective function as giving as below [50,51].

$$f_i(x) = \frac{f_i(x) - f_i^{min}(x)}{f_i^{max}(x) - f_i^{min}(x)}, \tag{27}$$

where $f_i^{max}(x)$ and $f_i^{min}(x)$ are the upper and lower boundaries of the ith individual objective function, respectively.

5. Energy Flow Modeling for SAPV System

In this research, the operation process of energy management of a SAPV is illustrated in Figure 5. The first step of the algorithm can be performed by obtaining the specification of the system such as the efficiency of PV module, efficiency of charging and discharging of the storage battery, the efficiency of the inverter, converter and wires.

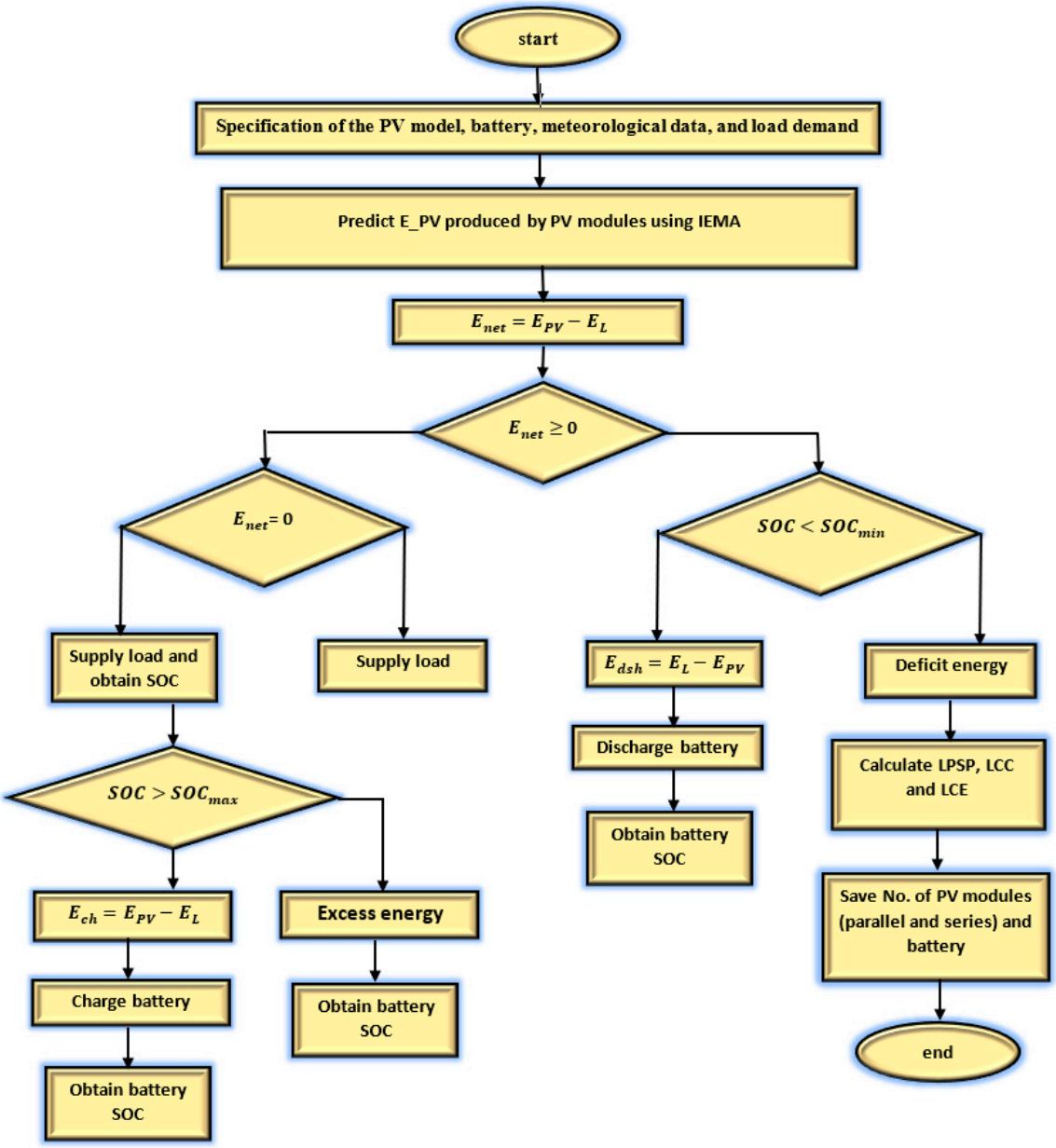

Figure 5. The flow chart of energy management of a SAPV system.

The simulation starts to calculate the E_net by subtracting the predicted output energy of the PV model from the energy of the load. Then, the net energy is classified in three cases which are:

- Case 1: The energy of PV array equals to the energy of the required load demand.
- Case 2: The energy of PV array is larger than the energy of the required load demand.
- Case 3: The energy of PV array is less than the energy of the required load demand.

In the first case, the battery energy is not used and there is no damped or deficit energy which is equal to zero. In the second case, the energy produced by PV array is larger than the load energy. There is an excess energy and depending on the state of charge of the battery (SOC). If the SOC of the battery is full, the amount of excess energy will be damped. In contrast, the amount of excess energy will be used to charge the battery and the new value of SOC will be calculated by Equation (9) and the deficit energy is zero. In case 3, if the SOC of the storage battery is more than the minimum value E_{bat_min} as in equation (10) then the storage battery is able to fulfill the load demand. The load will

be supplied with/without the energy of PV array and storage battery. Else if SOC of the battery is less than the minimum value, the system cannot meet the load demand and there is deficit energy. The three-objective function LLP, LCC, and LCE are calculated in each iteration.

6. Results and Discussion

In this paper, $AWPSO_{cf}$ and $SFPSO_{cf}$ are proposed for finding optimal configuration of the SAPV system. The hourly meteorological data for one year in Klang Valley recorded by Subang Meteorological Station is utilized in the optimization process with latitude (3.12°) north and longitude (101.6°) east. The meteorological data were obtained from a monitoring system that used solar radiation transmitter of high-stability silicon PV detector model WE300 with an accuracy of (± 1%), while the (± 0.25 °C) is the accuracy of the temperature sensor for the surface of the PV arrays of the same model, air temperature sensor model WE700 with an accuracy of (± 0.1 °C) and range (−50 °C–+50 °C), and current transducer model: CTH-050 with input and output range of (0–50 A (DC), and 4–20 mA) [52]. The proposed SAPV system is used to supply the load demand for house in a remote area. A typical household is illustrated in Figure 6. Annual hourly meteorological data of Kuala Lumpur city, Malaysia are obtained for this purpose. The monthly average of daily solar irradiation and ambient temperature are illustrated in Figure 7.

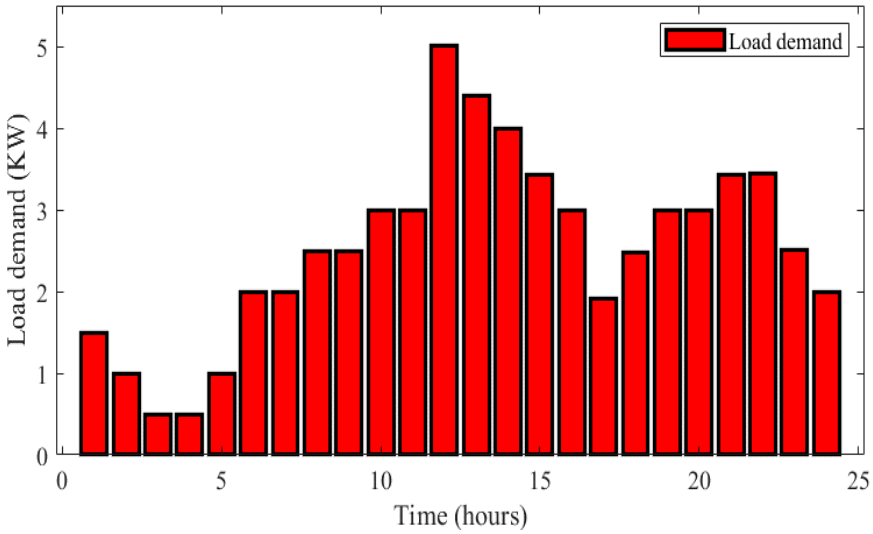

Figure 6. load demand of a typical house in remote area (KWh).

Figure 8 illustrates the correlation between the computed and experimental values of the current using Improved electromagnetism (IEM), slap swarm optimization (SSA), EM, repaired adaptive differential evolution (Rcr-IJADE) [53], adaptive differential evolution (IADE) [54], and penalty-based differential evolution (PDE) [55] algorithms. The results demonstrate that the IEM algorithm is very close the to the experimental values. Moreover, the RMSE value is small when the number of data set points is reduced. Finally, the IEM algorithm can predict the system's output energy accurately. Table 3. demonstrates the RMSE values of IEM compared with other methods. The bold face clarifies the minimum value of RMSE under seven weather conditions.

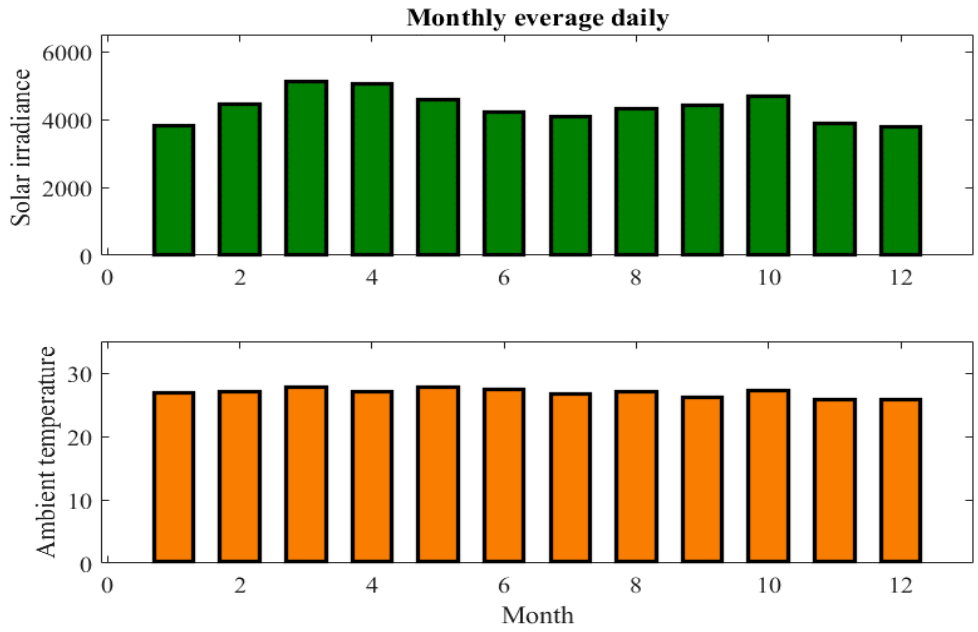

Figure 7. Monthly average of meteorological data in Malaysia.

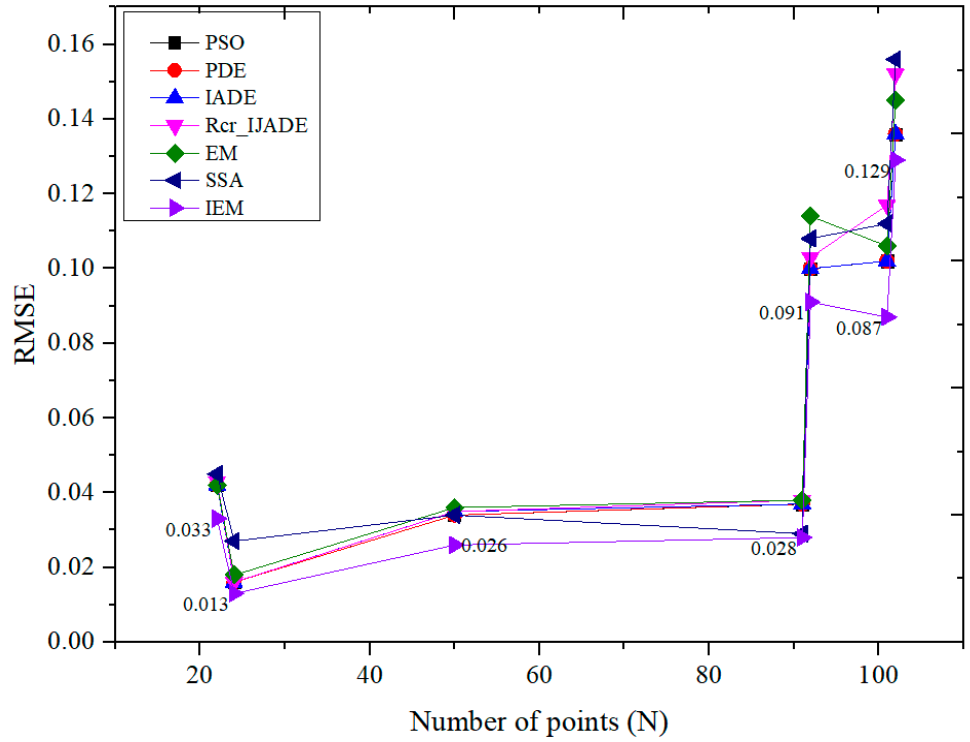

Figure 8. Root mean square error (RMSE) values of IEM, slap swarm optimization (SSA), EM, Rcr-IJADE, adaptive differential evolution (IADE), and penalty-based differential evolution (PDE) algorithms at various weather conditions.

Table 3. shows the root mean square error (RMSE) values of IEM, SSA, EM, Rcr-IJADE, IADE, and PDE algorithms.

Weather Condition	**S1**	**S2**	**S3**	**S4**	**S5**	**S6**	**S7**	**Average**
Length of Data Points (N)	**22**	**24**	**50**	**91**	**92**	**101**	**102**	
RMSE_PDE	0.042	0.016	0.034	0.037	0.100	0.102	0.136	0.0672
RMSE_IADE	0.042	0.016	0.035	0.037	0.100	0.102	0.136	0.0675
RMSE_Rcr-IJADE	0.043	0.016	0.035	0.038	0.107	0.113	0.116	0.0740
RMSE_EM	0.042	0.018	0.036	0.038	0.114	0.106	0.145	0.0716
RMSE_SSA	0.045	0.027	0.034	0.029	0.108	0.112	0.156	0.0734
RMSE_IEM	0.033	0.013	0.026	0.028	0.091	0.087	0.129	0.0589

In this study, three decision variables are obtained which are the parallel (N_p) and series N_s numbers of PV modules and the number of storage battery (*Bat*). For fair comparison, the search space of N_s and N_p decision variables is (4,80) and (4,60) for *Bat* are considered same in both $AWPSO_{cf}$ and $SFPSO_{cf}$ algorithms. The size of the population is set to be 50. On the other hand, the maximum number of iterations is set to 50 in order to clarify stability of optimal solutions. The value of $\varnothing$ is selected to be 2.

Figure 9 demonstrates the development of evaluation of aggregation function with maximum iteration of the proposed methods to optimize the size of SAPV system. The $SFPSO_{cf}$ has minimum f value which is 0.031249 at 12 generation. It can be observed that, the $SFPSO_{cf}$ and $AWPSO_{cf}$ algorithms have trivial difference between the fitness function values, which means that the two algorithms are very comparative.

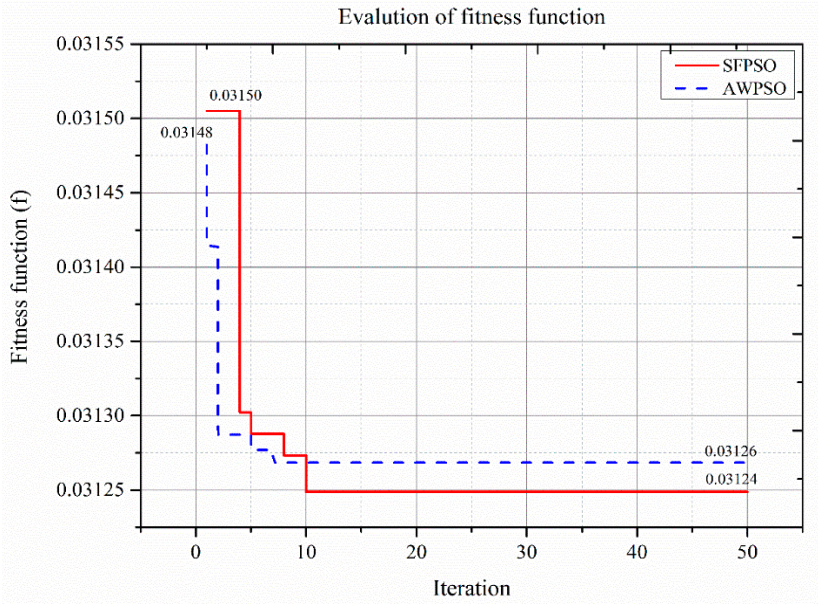

Figure 9. Evolution of aggregation function f for the $SFPSO_{cf}$ and $AWPSO_{cf}$ algorithms.

Table 4 indicates the initializing weights (W_1, W_2, W_3), total number of PV module (N), number of parallel module (N_p), number of series module (N_s), and number of storage battery (*Bat*). The range of weights sets are [1,9] with step size is 0.1. The acceptable level of LLP is less than 1%. The trade-off between the defined level of reliability and minimum cost are required in choosing an optimal configuration of a SAPV system. Thus, the optimal values of W_1, W_2, and W_3 are 0.4, 0.5, and 0.1 for $AWPSO_{cf}$ and $SFPSO_{cf}$ algorithms. The number of N_p, N_s and *Bat* are (47 and 60), (5 and 4), and (45,44) for the $SFPSO_{cf}$ and $AWPSO_{cf}$ algorithms, respectively. From Table 4, the $SFPSO_{cf}$ and $AWPSO_{cf}$ are very close to each other in terms of variables with bold face. The number of N PV module is increased

from 192 to 357 and 348 at end levels of optimization with various sets of weights, which means that the value of f strongly depends on the weight's value.

Table 4. Different weights sets and optimal configurations of the SAPV system.

Weights			SFPSO	AWPSO	SFPSO	AWPSO	SFPSO	AWPSO	SFPSO	AWPSO	SFPSO	AWPSO
W_1	W_2	W_3	N		N_s		N_p		*Bat*		Time	
0.1	0.8	0.1	192	192	32	4	6	48	32	32	89.39063	87.98438
0.1	0.5	0.4	268	224	67	14	4	16	29	33	85.84375	86.25
0.2	0.6	0.2	224	312	4	78	56	4	33	28	95.875	83.40625
0.2	0.5	0.3	264	264	22	66	12	4	31	31	97.48438	89.84375
0.3	0.6	0.1	224	224	4	4	56	56	38	38	95.23438	86.85938
0.3	0.4	0.3	294	300	42	4	7	75	32	32	96.28125	87.8125
0.4	0.5	0.1	235	240	47	60	5	4	45	44	88.5156	87.3125
0.5	0.4	0.1	252	297	18	33	14	9	42	36	84.78125	88.25
0.6	0.3	0.1	296	272	74	68	4	4	36	42	88.03125	88.71875
0.6	0.2	0.2	320	330	80	11	4	30	34	34	85.23438	90.20313
0.7	0.2	0.1	308	308	77	11	4	28	36	36	101.8281	88.96875
0.8	0.1	0.1	357	348	21	12	17	29	35	35	91.9375	93.73438

The performance results of the standalone PV system for the three objectives and fitness values are explained in Table 5. According to Table 5, the values of f, LLP, LCC, and LCE are [0.031249 and 0.031268], [0.002431 and 0.002361], [53167 and 53642] USD, and [1.6413 and 1.6214] USD for the $SFPSO_{cf}$ and $AWPSO_{cf}$ algorithms, respectively. From results, the value of the f for $SFPSO_{cf}$ algorithm is less than $SFPSO_{cf}$ algorithm by a trivial value. The maximum f value registered for two algorithms are 0.0468 and 0.0475 at set of weights [0.1, 0.5, 0.4] and [0.2, 0.6, 0.2], respectively. In contrast, the minimum f value registered are 0.011215 and 0.01122 at set of weights [0.8, 0.1, 0.1] for $SFPSO_{cf}$ and $AWPSO_{cf}$ algorithms. It's worth to note that increasing the value of weight is directly proportional to the relative individual objective and inversely proportional to the decreasing value of weight. The LLP value is dramatically decreased from 0.038 at $W_1 = 1$ to zero and 0.00007 at $W_1 = 8$ for the two algorithms corresponding with increasing LLC value as the number of N and Bat increased. The LCE is directly affected by the given weight value which is chosen to be high because of the balance between LLP and LCC objectives.

Table 5. Different weights sets and optimal performance of the SAPV system.

Weights			SFPSO	AWPSO	SFPSO	AWPSO	SFPSO	AWPSO	SFPSO	AWPSO
W_1	W_2	W_3	f		LLP		LCC		LCE	
0.1	0.8	0.1	0.0389	0.0389	0.031883	0.0318	43,018.2152	43,018.2152	1.6254	1.6254
0.1	0.5	0.4	0.0468	0.0405	0.012971	0.0137	53,667.7754	48,137.1618	1.4527	1.5590
0.2	0.6	0.2	0.0405	0.0475	0.013756	0.0113	48,137.1618	60,040.0288	1.5590	1.3960
0.2	0.5	0.3	0.0423	0.0423	0.008764	0.0087	53,624.0686	53,624.0686	1.4735	1.4735
0.3	0.6	0.1	0.0350	0.0350	0.008638	0.0086	49,539.8948	49,539.8948	1.6044	1.6044
0.3	0.4	0.3	0.0381	0.0381	0.003987	0.0035	58,440.61522	59,347.8152	1.4420	1.4351
0.4	0.5	0.1	0.0312	0.0312	0.002431	0.0023	53,166.9210	53,642.3745	1.6413	1.6214
0.5	0.4	0.1	0.0268	0.0277	0.001992	0.0009	54,895.6812	60,016.4016	1.5803	1.4659
0.6	0.3	0.1	0.0220	0.0221	0.000984	0.0007	59,865.2016	57,919.6813	1.4672	1.5448
0.6	0.2	0.2	0.0223	0.0223	0.000876	0.0006	62,932.9084	64,444.9084	1.4267	1.4167
0.7	0.2	0.1	0.0168	0.0168	0.000589	0.0005	61,679.6016	61,679.6016	1.4528	1.4528
0.8	0.1	0.1	0.0112	0.0112	0	0	68,807.8550	67,447.0550	1.3982	1.4060

Figure 10 shows the development of N and *Bat* with generation for $SFPSO_{cf}$ and $AWPSO_{cf}$ algorithms based on optimal configuration which is denoted by bold face in Tables 4 and 5. Figure 11 demonstrates the optimal configuration of the two algorithms at all sets of weights for N and *Bat* with favourable level of LLP value.

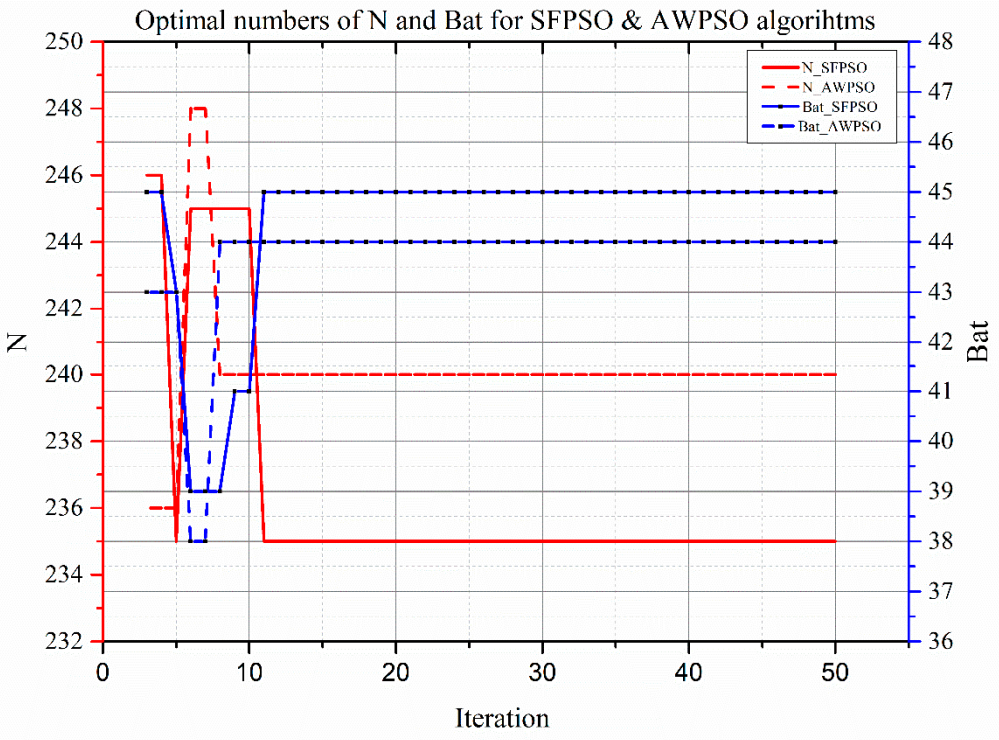

Figure 10. Evolution of optimal *N* and *Bat* for $SFPSO_{cf}$ and $AWPSO_{cf}$ algorithms.

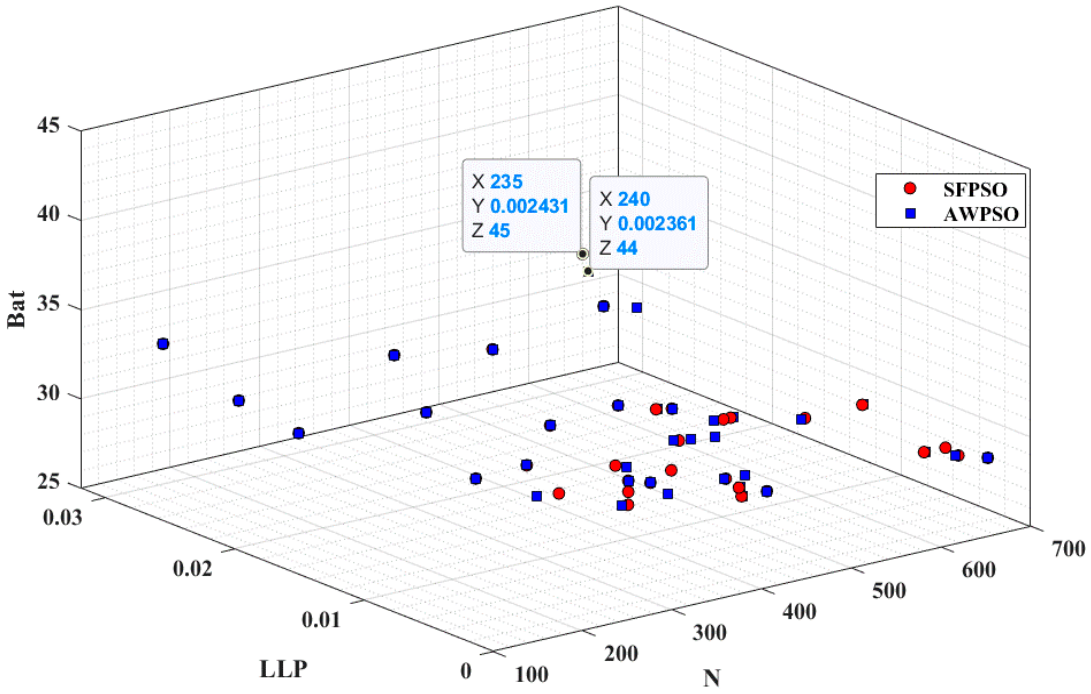

Figure 11. Evaluation of *N* and *Bat* at desired level of loss of load probability (LLP) value with different weights sets.

Figure 12 is graphed of swarm's motion in 50 particles generations which can be viewed that 50 particles fly from different sets weights. During the optimization process, the particle best and global best will be adapted until achieving high reliability and minimum cost at N = 235 and 240 and Bat = 45 and 44, respectively. The chosen point is called global best that combine the three objectives domain which is a complex task in designing such system. It can be noticed from Figure 12 that particles

become close to each other and the convergence is reached to the optimal value for the two $SFPSO_{cf}$ and $AWPSO_{cf}$ algorithms.

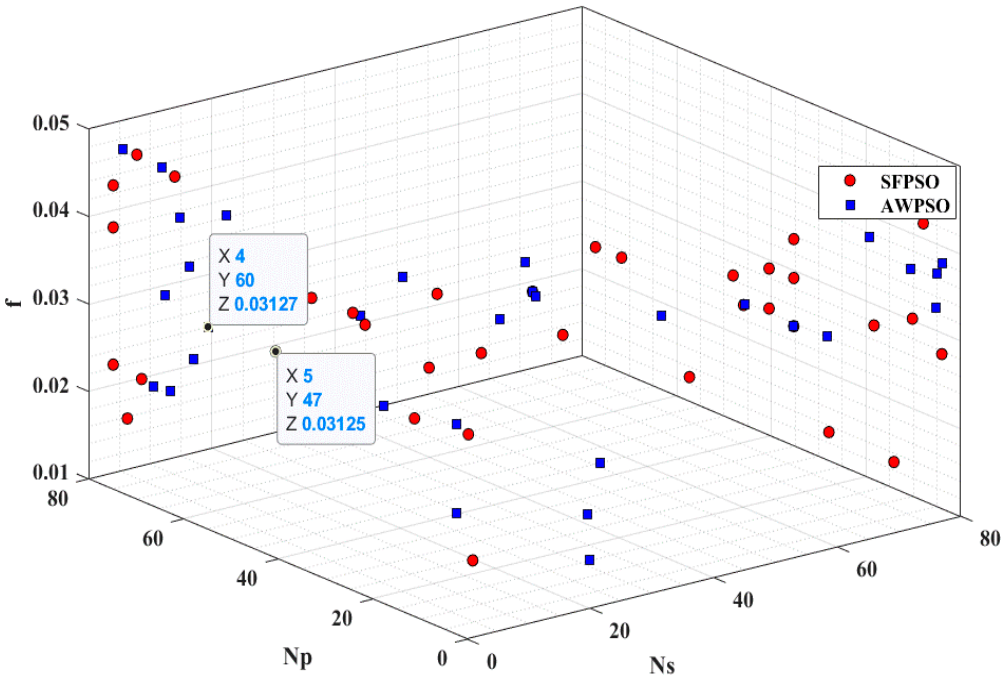

Figure 12. Evaluation of N_s, N_p, and f value with different weights sets.

From Figure 13, the optimal configurations based on $SFPSO_{cf}$ and $AWPSO_{cf}$ algorithms are close to each other with small difference in the three objectives because of the variation in values of inertia weights during the optimization. It is worth to mentioned that the results for the independent runs can guarantee to convergence to the same optimal fitness value which shows the reliability of proposed two algorithms.

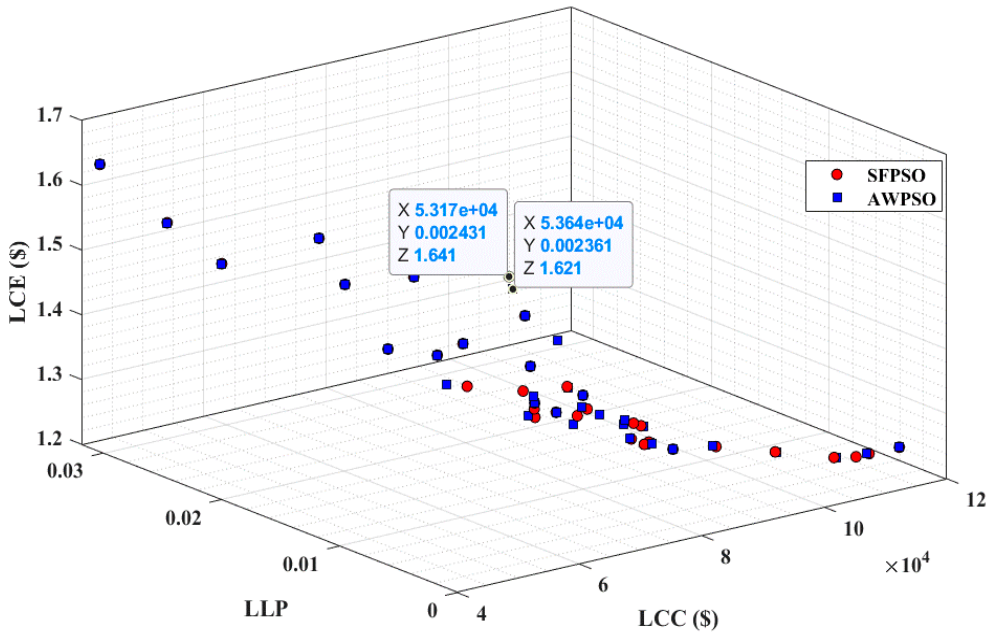

Figure 13. Evaluation of life cycle cost (LCC), LLP, and levelized cost of energy (LCE) values with different weights sets.

However, the drawbacks of aggregation method are that identify only one solution based on given weights for each individual objective. Furthermore, the weights initialization, which are aggregated by the aggregation function, is the main obstacle of aggregation method. It is worth mentioning that the results of the optimization problem that solved by aggregation method strongly depends on the weights. Therefore, other method can be proposed to overcome the limitations of the proposed method, and other nonlinear individual objective functions can be suggested and added for aggregation function as future work.

The results of the proposed methods for sizing of a SAPV system are validated by results of the numerical method to demonstrate the accuracy of the presented two methods. The range of the search space are defined by using intuitive method for every possible N_s, N_p, and *Bat* within range (1,40), (1,40) and (1,50), respectively. The desired value for LLP is larger than 0.001. some of optimal configurations based on numerical method that corresponding to the results of the $SFPSO_{cf}$ and $AWPSO_{cf}$ algorithms are tabulated in Table 6. It's clear that the numerical method is almost able to meet the optimal configurations of the two mentioned methods except that it's over the range of search space of the numerical method as well as if the optimal configuration exceeds the LLP value. The execution time by using numerical method is 10,295.7187 s and the number of configurations is 59,503. Therefore, a high consistency has been achieved for the two proposed methods when their compared with iterative method.

Table 6. Sets of optimal configurations for sizing of the SAPV system using numerical method.

N	N_s	N_p	*Bat*	LLP	LLC	LCE	Def E	Excess E	Cost Year
192	16	12	32	0.0318	43,018.2152	1.6254	710.9272	5883.6877	2150.9107
224	8	28	33	0.0137	48,137.1618	1.5590	306.7182	10,340.8241	2406.8580
250	25	10	32	0.0092	51,787.8152	1.5028	206.7034	14,112.5849	2589.3907
264	22	12	31	0.0087	53,624.0686	1.4735	195.4137	16,250.9898	2681.2034
224	7	32	38	0.0086	49,539.8948	1.6044	192.6142	10,234.6940	2476.9947
306	9	34	29	0.0079	59,413.3754	1.4085	178.0643	22,429.1878	2970.6687
230	10	23	38	0.0072	50,447.0948	1.5912	162.5026	11,191.2996	2522.3547
294	14	21	32	0.0039	58,440.6152	1.4420	88.9030	20,576.5615	2922.0307
240	15	16	44	0.0023	53,642.3744	1.6214	52.6528	12,539.9811	2682.1187
252	18	14	42	0.0019	54,895.6812	1.5803	44.4125	14,227.6421	2744.7840

The operation performance of the standalone PV system is analysed based on N_s = 5, N_p = 47 and *Bat* = 45 of the $SFPSO_{cf}$ algorithm as it has lower f than the $AWPSO_{cf}$ algorithm. Two methods are selected based on maximum and minimum solar radiation to show the performance of the system. The first month is based on the maximum solar radiation which was accrued in March. The monthly average daily solar radiation of about 5131.5 W/m^2. The energy generated by the PV modules is about 3000.2154 KWh and the deficit energy is about 0 KWh. Therefore, the LLP value is 0, LCC is 53,167 USD and LCE is 16.5348 USD. The hourly performance of the proposed SAPV system of maximum solar radiation is illustrated in Figure 14.

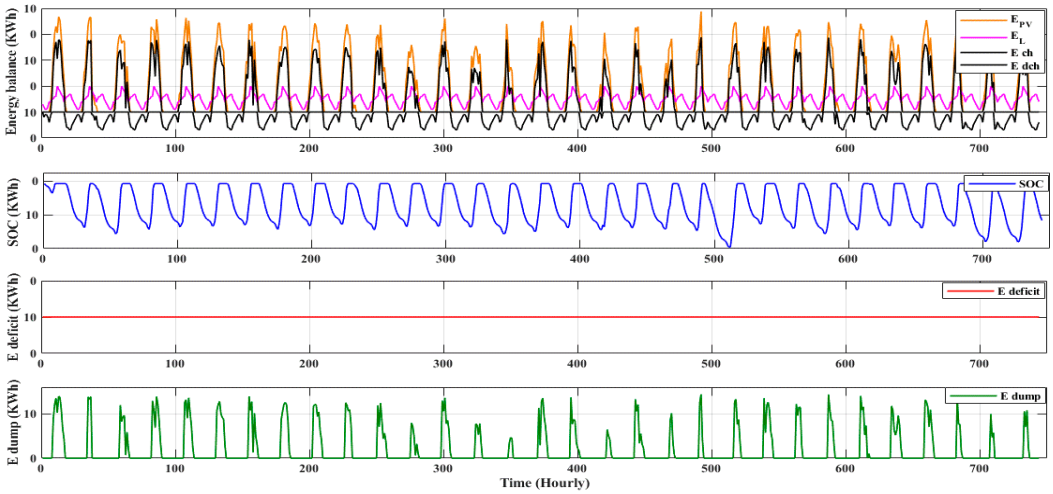

Figure 14. Performance of the SAPV system based on chosen optimal configuration in March.

Whilst, the minimum solar radiation was registered in December. The monthly average daily solar radiation of about 3779.8 W/m^2. The energy conducted by the PV modules is 4447.0 KWh and the deficit energy in this month is 20.18 KWh. Thus, the LLP value is 0.0191, LCC is 53,167 USD and LCE is 22.1186 USD. The hourly performance of the proposed SAPV system of minimum solar radiation is illustrated in Figure 15.

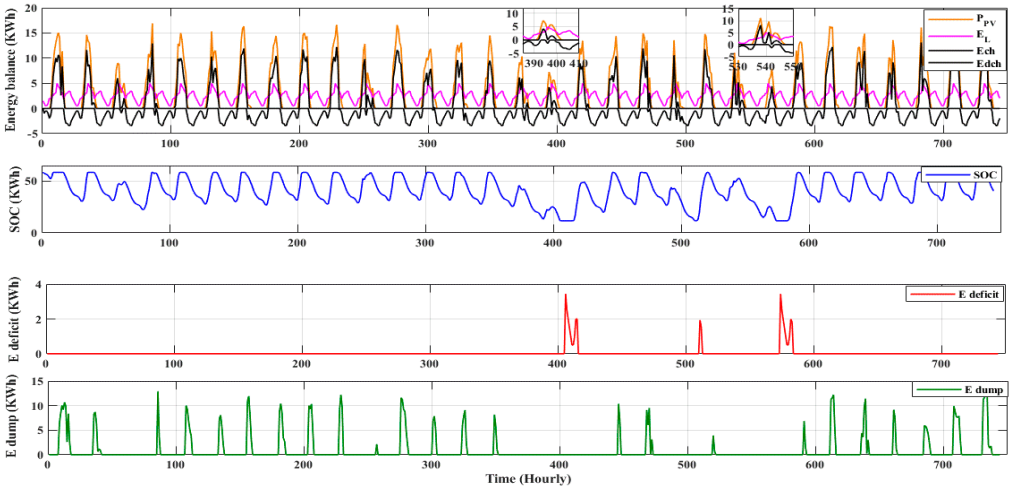

Figure 15. Performance of the SAPV system based on chosen optimal configuration in December.

According to Figures 14 and 15, we can observe that the energy conducted by the PV array are strongly dependent on the availability of the meteorological data. Thus, in March the SOC of the battery is almost at maximum values. Whilst, the SOC in December exceeded the minimum values of the storage battery in only three days. The monthly average daily performance of the proposed SAPV system throughout one year based on optimal configuration can be given in Table 7. The proposed algorithm $AWPSO_{cf}$ exhibits excellent performance results in term of reliability, cost-effective, and CPU-execution time. From Table 7, the difference between the conducted energy by PV modules, deficit energy, and dump energy are reasonable and promising for real investment of the SAPV system especially in rural area.

Table 7. shows monthly average daily performance of the SAPV system under optimal solutions.

Month	Jan	Feb	Mar	Apr	May	Jun	Jul	Aug	Sep	Oct	Nov	Dec
P_PV (KWh)	78.60	90.21	103.72	101.96	93.09	86.58	83.98	87.80	89.88	95.41	79.46	77.53
E deficit (KWh)	0.27	0.14	0	0	0	0	0.17	0	0	0	0	1.16
E dump (KWh)	22.91	33.57	47.78	45.06	37.52	30.20	26.30	32.08	34.36	37.89	23.42	21.29

7. Conclusions

In this research, $SFPSO_{cf}$ and $AWPSO_{cf}$ methods for optimally sizing SAPV system were proposed. Three constraint objectives are utilized as techno-economic criteria which are normalized, weighted, and then aggregated by mono-objective function. The optimum design was chosen by minimizing objective function based on LLP, LCC, and LCE criteria. The results showed the superiority of $SFPSO_{cf}$ in term of accuracy which has minimum objective function with value 0.031249. The optimal configuration of SAPV system for $SFPSO_{cf}$ method was 5 connected in series and 47 in parallel, respectively. The number of storage battery was 45. The performance was analysed for one year using hourly meteorological data in Malaysia. The LLP value is 0.002431, LCC is 53,166.9 USD and LCE is 1.6431 USD. March and December, the months of the maximum and the minimum solar radiation periods, respectively, were selected to show the operational performance of SAPV system. The results of operational performance show high reliability of the standalone PV system; hence, the acceptable level of LLP value is less than 1%.

Author Contributions: C.G. and H.H. were involved in the paper editing and reviewing, conceptualization, investigation, and supervision. H.M.R. collected the data, methodology, software implementation, and writing original draft. M.A. and H.M.R. conducted formal analysis, conceptualization, and investigation. All authors have read and agreed to the published version of the manuscript.

Funding: This research received no external funding.

Conflicts of Interest: The author declares that there is no conflict of interest regarding the publication of this paper.

References

1. Dawoud, S.M.; Lin, X.; Okba, M.I. Hybrid renewable microgrid optimization techniques: A review. *Renew. Sustain. Energy Rev.* **2018**, *82*, 2039–2052. [CrossRef]
2. Ayop, R.; Isa, N.M.; Tan, C.W. Components sizing of photovoltaic stand-alone system based on loss of power supply probability. *Renew. Sustain. Energy Rev.* **2018**, *81*, 2731–2743. [CrossRef]
3. Kumar, A.; Singh, A.R.; Deng, Y.; He, X.; Kumar, P.; Bansal, R.C. A Novel Methodological Framework for the Design of Sustainable Rural Microgrid for Developing Nations. *IEEE Access* **2018**, *6*, 24925–24951. [CrossRef]
4. Khalilpour, R.; Vassallo, A. Leaving the grid: An ambition or a real choice? *Energy Policy* **2015**, *82*, 207–221. [CrossRef]
5. Bazilian, M.; Onyeji, I.; Liebreich, M.; MacGill, I.; Chase, J.; Shah, J.; Gielen, D.; Arent, D.; Landfear, D.; Zhengrong, S. Re-considering the economics of photovoltaic power. *Renew. Energy* **2013**, *53*, 329–338. [CrossRef]
6. Khatib, T.; Ibrahim, I.A.; Mohamed, A. A review on sizing methodologies of photovoltaic array and storage battery in a standalone photovoltaic system. *Energy Convers. Manag.* **2016**, *120*, 430–448. [CrossRef]
7. Rawat, R.; Kaushik, S.; Lamba, R. A review on modeling, design methodology and size optimization of photovoltaic based water pumping, standalone and grid connected system. *Renew. Sustain. Energy Rev.* **2016**, *57*, 1506–1519. [CrossRef]
8. Mandelli, S.; Barbieri, J.; Mereu, R.; Colombo, E. Off-grid systems for rural electrification in developing countries: Definitions, classification and a comprehensive literature review. *Renew. Sustain. Energy Rev.* **2016**, *58*, 1621–1646. [CrossRef]
9. Chel, A.; Tiwari, G.; Chandra, A. Simplified method of sizing and life cycle cost assessment of building integrated photovoltaic system. *Energy Build.* **2009**, *41*, 1172–1180. [CrossRef]
10. Ghafoor, A.; Munir, A. Design and economics analysis of an off-grid PV system for household electri fi cation. *Renew. Sustain. Energy Rev.* **2015**, *42*, 496–502. [CrossRef]

11. Jakhrani, A.Q.; Othman, A.-K.; Rigit, A.R.H.; Samo, S.R.; Kamboh, S.A. A novel analytical model for optimal sizing of standalone photovoltaic systems. *Energy* **2012**, *46*, 675–682. [CrossRef]
12. Bortolini, M.; Gamberi, M.; Graziani, A.; Pilati, F. Economic and environmental bi-objective design of an off-grid photovoltaic–battery–diesel generator hybrid energy system. *Energy Convers. Manag.* **2015**, *106*, 1024–1038. [CrossRef]
13. Huang, B.-J.; Hou, T.-F.; Hsu, P.-C.; Lin, T.-H.; Chen, Y.-T.; Chen, C.-W.; Li, K.; Lee, K. Design of direct solar PV driven air conditioner. *Renew. Energy* **2016**, *88*, 95–101. [CrossRef]
14. Chen, S.-G. An efficient sizing method for a stand-alone PV system in terms of the observed block extremes. *Appl. Energy* **2012**, *91*, 375–384. [CrossRef]
15. Mandelli, S.; Brivio, C.; Colombo, E.; Merlo, M. A sizing methodology based on Levelized Cost of Supplied and Lost Energy for off-grid rural electrification systems. *Renew. Energy* **2016**, *89*, 475–488. [CrossRef]
16. Nordin, N.D.; Rahman, H.A. A novel optimization method for designing stand alone photovoltaic system. *Renew. Energy* **2016**, *89*, 706–715. [CrossRef]
17. Sarhan, A.; Hizam, H.; Mariun, N.; Ya'acob, M.E. An improved numerical optimization algorithm for sizing and configuration of standalone photo-voltaic system components in Yemen. *Renew. Energy* **2018**, *134*, 1434–1446. [CrossRef]
18. Dufo-López, R.; Lujano-Rojas, J.M.; Bernal-Agustín, J.L. Comparison of different lead–acid battery lifetime prediction models for use in simulation of stand-alone photovoltaic systems. *Appl. Energy* **2014**, *115*, 242–253. [CrossRef]
19. Erdinc, O.; Paterakis, N.G.; Pappi, I.N.; Bakirtzis, A.G.; Catalão, J.P.S. A new perspective for sizing of distributed generation and energy storage for smart households under demand response. *Appl. Energy* **2015**, *143*, 26–37. [CrossRef]
20. Makhloufi, S. Comparative study between classical methods and genetic algorithms for sizing remote PV systems. *Int. J. Energy Environ. Eng.* **2015**, *6*, 221–231. [CrossRef]
21. Mohamed, A.F.; Elarini, M.M.; Othman, A.M. A new technique based on Artificial Bee Colony Algorithm for optimal sizing of stand-alone photovoltaic system. *J. Adv. Res.* **2013**, *5*, 397–408. [CrossRef] [PubMed]
22. Khatib, T.; Elmenreich, W. An Improved Method for Sizing Standalone Photovoltaic Systems Using Generalized Regression Neural Network. *Int. J. Photoenergy* **2014**, *2014*, 1–8. [CrossRef]
23. Ben Salah, C.; Lamamra, K.; Fatnassi, A. New optimally technical sizing procedure of domestic photovoltaic panel/battery system. *J. Renew. Sustain. Energy* **2015**, *7*, 13134. [CrossRef]
24. Aziz, N.I.A.; Sulaiman, S.I.; Shaari, S.; Musirin, I.; Sopian, K. Optimal sizing of stand-alone photovoltaic system by minimizing the loss of power supply probability. *Sol. Energy* **2017**, *150*, 220–228. [CrossRef]
25. Alsadi, S.; Khatib, T. Photovoltaic Power Systems Optimization Research Status: A Review of Criteria, Constrains, Models, Techniques, and Software Tools. *Appl. Sci.* **2018**, *8*, 1761. [CrossRef]
26. Sadio, A.; Mbodji, S.; Fall, I. New numerical sizing approach of a standalone photovoltaic power at Ngoundiane, Senegal. *EAI Endorsed Trans. Energy Web* **2018**, *5*, 153814. [CrossRef]
27. Esfahani, I.J.; Yoo, C. An optimization algorithm-based pinch analysis and GA for an off-grid batteryless photovoltaic-powered reverse osmosis desalination system. *Renew. Energy* **2016**, *91*, 233–248. [CrossRef]
28. Habib, A.H.; Disfani, V.R.; Kleissl, J.; De Callafon, R.A. Optimal switchable load sizing and scheduling for standalone renewable energy systems. *Sol. Energy* **2017**, *144*, 707–720. [CrossRef]
29. Ibrahim, I.A.; Khatib, T.; Mohamed, A. Optimal sizing of a standalone photovoltaic system for remote housing electrification using numerical algorithm and improved system models. *Energy* **2017**, *126*, 392–403. [CrossRef]
30. Muhsen, D.H.; Nabil, M.; Haider, H.T.; Khatib, T. A novel method for sizing of standalone photovoltaic system using multi-objective differential evolution algorithm and hybrid multi-criteria decision making methods. *Energy* **2019**, *174*, 1158–1175. [CrossRef]
31. Benavente, F.; Lundblad, A.; Campana, P.E.; Zhang, Y.; Cabrera, S.; Lindbergh, G. Photovoltaic/battery system sizing for rural electrification in Bolivia: Considering the suppressed demand effect. *Appl. Energy* **2019**, *235*, 519–528. [CrossRef]
32. Lot, H.; Khodaei, A. Hybrid AC / DC microgrid planning. *Energy* **2017**, *118*, 37–46.
33. Lupangu, C.; Bansal, R. A review of technical issues on the development of solar photovoltaic systems. *Renew. Sustain. Energy Rev.* **2017**, *73*, 950–965. [CrossRef]

34. Chenlo, F.; Fabero, F.; Alonso, M.C. A comparative study between indoor and outdoor measurements, 1995; Final Report of Project: Testing, Norms, Reliability and Harmonisation. Joule II—-Contract N. JOU2-CT92-0178.
35. Arab, A.H.; Chenlo, F.; Benghanem, M. Loss-of-load probability of photovoltaic water pumping systems. *Sol. Energy* **2004**, *76*, 713–723. [CrossRef]
36. Northern Arizona Wind & Sun. Available online: https://www.solar-electric.com/centennial-gc2200p-flooded-deep-cycle-battery.html (accessed on 11 November 2019).
37. Ismail, M.; Moghavvemi, M.; Mahlia, T. Techno-economic analysis of an optimized photovoltaic and diesel generator hybrid power system for remote houses in a tropical climate. *Energy Convers. Manag.* **2013**, *69*, 163–173. [CrossRef]
38. Kazem, H.A.; Khatib, T.; Sopian, K. Sizing of a standalone photovoltaic/battery system at minimum cost for remote housing electrification in Sohar, Oman. *Energy Build.* **2013**, *61*, 108–115. [CrossRef]
39. Sidrach-De-Cardona, M.; López, L.M. A general multivariate qualitative model for sizing stand-alone photovoltaic systems. *Sol. Energy Mater. Sol. Cells* **1999**, *59*, 185–197. [CrossRef]
40. Muhsen, D.H.; Ghazali, A.B.; Khatib, T. Multiobjective differential evolution algorithm-based sizing of a standalone photovoltaic water pumping system. *Energy Convers. Manag.* **2016**, *118*, 32–43. [CrossRef]
41. Groumpos, P.; Papageorgiou, G. An optimal sizing method for stand-alone photovoltaic power systems. *Sol. Energy* **1987**, *38*, 341–351. [CrossRef]
42. Hosseinalizadeh, R.; Shakouri, H.; Amalnick, M.S.; Taghipour, P. Economic sizing of a hybrid (PV–WT–FC) renewable energy system (HRES) for stand-alone usages by an optimization-simulation model: Case study of Iran. *Renew. Sustain. Energy Rev.* **2016**, *54*, 139–150. [CrossRef]
43. Morningstar PS-MPPT-40 ProStar MPPT 40 Amp Solar Charge Controller. Available online: https://www.solar-electric.com/morningstar-prostar-mppt-controller-ps-mppt-40.html (accessed on 11 November 2019).
44. Lazou, A.A.; Papatsoris, A.D. The economics of photovoltaic stand-alone residential households: A case study for various European and Mediterranean locations. *Sol. Energy Mater. Sol. Cells* **2000**, *62*, 411–427. [CrossRef]
45. Yang, H.; Lu, L.; Zhou, W. A novel optimization sizing model for hybrid solar-wind power generation system. *Sol. Energy* **2007**, *81*, 76–84. [CrossRef]
46. Kennedy, J.; Eberhart, R. Particle Swarm Optimization. In Proceedings of the ICNN'95—International Conference on Neural Networks, Perth, WA, Australia, 27 November–1 December 1995; Volume 4, pp. 1942–1948.
47. Kerdphol, T.; Fuji, K.; Mitani, Y.; Watanabe, M.; Qudaih, Y. Optimization of a battery energy storage system using particle swarm optimization for stand-alone microgrids. *Int. J. Electr. Power Energy Syst.* **2016**, *81*, 32–39. [CrossRef]
48. Kornelakis, A.; Marinakis, Y. Contribution for optimal sizing of grid-connected PV-systems using PSO. *Renew. Energy* **2010**, *35*, 1333–1341. [CrossRef]
49. Luna-Rubio, R.; Trejo-Perea, M.; Vargas-Vázquez, D.; Ríos-Moreno, G. Optimal sizing of renewable hybrids energy systems: A review of methodologies. *Sol. Energy* **2012**, *86*, 1077–1088. [CrossRef]
50. Talbi, E.G.T. *Metaheuristics: From Design to Implementation*; John Wiley & Sons, Inc.: Hoboken, NJ, USA, 2009.
51. Jakob, W.; Blume, C. Pareto Optimization or Cascaded Weighted Sum: A Comparison of Concepts. *Algorithms* **2014**, *7*, 166–185. [CrossRef]
52. Muhsen, D.H.; Ghazali, A.B.; Khatib, T.; Abed, I.A.; Natsheh, E.M. Sizing of a standalone photovoltaic water pumping system using a multi-objective evolutionary algorithm. *Energy* **2016**, *109*, 961–973. [CrossRef]
53. Gong, W.; Cai, Z. Parameter extraction of solar cell models using repaired adaptive differential evolution. *Sol. Energy* **2013**, *94*, 209–220. [CrossRef]
54. Jiang, L.L.; Maskell, D.L.; Patra, J.C. Parameter estimation of solar cells and modules using an improved adaptive differential evolution algorithm. *Appl. Energy* **2013**, *112*, 185–193. [CrossRef]
55. Ishaque, K.; Salam, Z.; Mekhilef, S.; Shamsudin, A. Parameter extraction of solar photovoltaic modules using penalty-based differential evolution. *Appl. Energy* **2012**, *99*, 297–308. [CrossRef]